THE JOURNAL OF BIOLOGICAL CHEMISTRY VOL. 287, NO. 21, pp. 17682–17692, May 18, 2012

Tyrosine-phosphorylated Caveolin-1 (Tyr-14) Increases Sensitivity to Paclitaxel by Inhibiting BCL2 and BCLxL Proteins via c-Jun N-terminal Kinase (JNK)*

Received for publication, September 13, 2011, and in revised form, February 24, 2012 Published, JBC Papers in Press, March 20, 2012, DOI 10.1074/jbc.M111.304022

Ayesha N. Shajahan[1], **Zachary C. Dobbin, F. Edward Hickman, Sivanesan Dakshanamurthy, and Robert Clarke**

From the Department of Oncology, Lombardi Comprehensive Cancer Center, Georgetown University, Washington, D. C. 20057

Background: Phosphorylation of caveolin-1 (CAV1) on Tyr-14 facilitates apoptosis by inactivating BCL2 in response to paclitaxel.
Results: Wild-type CAV1 (wtCAV1), but not the phosphorylation-deficient mutant (Y14F), inactivates BCL2 and BCLxL through activation of JNK.
Conclusion: Inhibition of CAV1 phosphorylation confers paclitaxel resistance because it cannot inhibit BCL2 and BCLxL.
Significance: Knowledge of CAV1 variant-specific function is necessary to determine its precise role(s) in cancer progression.

Paclitaxel, an anti-microtubule agent, is an effective chemotherapeutic drug in breast cancer. Nonetheless, resistance to paclitaxel remains a major clinical challenge. The need to better understand the resistant phenotype and to find biomarkers that could predict tumor response to paclitaxel is evident. In estrogen receptor α-positive (ER$^+$) breast cancer cells, phosphorylation of caveolin-1 (CAV1) on Tyr-14 facilitates mitochondrial apoptosis by increasing BCL2 phosphorylation in response to low dose paclitaxel (10 nM). However, two variants of CAV1 exist: the full-length form, CAV1α (wild-type CAV1 or wtCAV1), and a truncated form, CAV1β. Only wtCAV1 has the Tyr-14 region at the N terminus. The precise cellular functions of CAV1 variants are unknown. We now show that CAV1 variants play distinct roles in paclitaxel-mediated cell death/survival. CAV1β expression is increased in paclitaxel-resistant cells when compared with sensitive cells. Expression of CAV1β in sensitive cells significantly reduces their responsiveness to paclitaxel. These activities reflect an essential role for Tyr-14 phosphorylation because wtCAV1 expression, but not a phosphorylation-deficient mutant (Y14F), inactivates BCL2 and BCLxL through activation of c-Jun N-terminal kinase (JNK). MCF-7 cells that express Y14F are resistant to paclitaxel and are resensitized by co-treatment with ABT-737, a BH3-mimetic small molecule inhibitor. Using structural homology modeling, we propose that phosphorylation on Tyr-14 enables a favorable conformation for proteins to bind to the CAV1 scaffolding domain. Thus, we highlight novel roles for CAV1 variants in cell death; wtCAV1 promotes cell death, whereas CAV1β promotes cell survival by preventing inactivation of BCL2 and BCLxL via JNK in paclitaxel-mediated apoptosis.

Paclitaxel (Taxol) is a microtubule-polymerizing agent widely used in combination with anthracyclines or alkylating agents, which improves both overall survival and disease-free survival in metastatic breast cancer (1, 2). Paclitaxel is also used in the management of early-stage breast cancer. Although the response rate for paclitaxel is 25–69% when used as first-line treatment, drug resistance is common (3). Both intrinsic and acquired resistance to paclitaxel can result from multiple factors including changes in signaling associated with apoptosis or programmed cell death (4). Apoptosis is initiated either by death receptor activation, leading to induction of the *extrinsic pathway*, or at the mitochondria by the *intrinsic or mitochondrial pathway* (5). Because the BCL2 family of proteins regulates the integrity of the outer mitochondrial membrane, and hence the mitochondrial pathway of apoptosis, targeting the anti-apoptotic function of BCL2 in drug-resistant cancer cells is a rational strategy to restore the normal apoptotic processes.

The caveolin (CAV)[2] family of proteins is composed of three isoforms: CAV1, -2, and -3 (6, 7). CAV1 is a 178-amino acid protein that exists as two variants. The wild type (hereafter referred to as wtCAV) is the full-length protein, and CAV1α contains residues 1–178. CAV1β contains only residues 32–178 (see Fig. 1*A*) and is formed by translation initiation from the second AUG codon (7, 8). Although both wtCAV1 and CAV1β are co-expressed in most human cells, only wtCAV1 can be phosphorylated on Tyr-14 by Src, Abl, or Fyn (9, 10). CAV1 is an integral membrane protein that can be localized in multiple cellular domains (11–13). CAV1 expression during breast tumorigenesis is compartment- and stage-specific (6, 14). Although the role of CAV1 as a tumor suppressor is controversial (15, 16), its role as an essential *modulator* of tumorigenesis is well accepted (6, 7, 13, 16). In breast cancer cell mod-

* This work was supported, in whole or in part, by National Institutes of Health Grant U54-CA149147 (to R. C.) from the USPHS. This work was also supported by a Susan G. Komen for the Cure Fellowship (PDF0600477) and American Cancer Society Institutional Research Grant IRG 92-152-17 (to A. N. S.).
[1] To whom correspondence should be addressed: 3970 Reservoir Rd., NW, NRB W405B, Washington, D. C. 20057. Tel.: 202-687-4060; Fax: 202-687-7505; E-mail: ans33@georgetown.edu.

[2] The abbreviations used are: CAV1, caveolin-1; CSD, CAV1 scaffolding domain; ABT-737, 4-[4-[(4′-chloro[1,1′-biphenyl]-2-yl)methyl]-1-piperazinyl]-N-[[4-[[(1R)-3-(dimethylamino)-1-[(phenylthio)methyl]propyl]-amino]-3-nitrophenyl]sulfonyl]benzamide; BCL2, B-cell lymphoma 2; BCLxL, B-cell lymphoma extra large; ER$^+$, estrogen receptor α-positive; SP600125, anthra[1,9-cd]pyrazol-6(2*H*)-one,1,9-pyrazoloanthrone; wtCVA1, wild-type caveolin-1; Y14p, phosphorylated Tyr-14; EV, empty vector; PARP, poly(ADP-ribose) polymerase-2.

els, CAV1 is down-regulated in cells with a noninvasive phenotype, but it is overexpressed in cells with an invasive phenotype (6, 7, 15, 16). To date, work on CAV1 in breast cancer had focused on *total* CAV1 expression, but the specific roles of wtCAV1 *versus* CAV1β had remained unknown. In zebrafish, CAV1 variants play distinct roles in development, particularly in actin cytoskeleton organization (17). Here we establish a novel role for CAV1β in conferring resistance to paclitaxel in ER^+ breast cancer cells by preventing inactivation of BCL2 and BCLxL.

Tyrosine phosphorylation of CAV1 on Tyr-14 is an essential determinant of paclitaxel responsiveness in breast cancer cells (18), and expression of a phosphorylation-deficient mutant, Y14F, prevents the paclitaxel-mediated increase in mitochondrial apoptosis. We now show that paclitaxel-resistant MCF-7 (ER^+) breast cancer cells show increased expression of the CAV1β isoform that lacks Tyr-14 when compared with wtCAV1/CAV1α. Moreover, expression of CAV1β in sensitive MCF-7 cells decreased their sensitivity to paclitaxel when compared with expression of wtCAV1. To understand how tyrosine phosphorylation on Tyr-14 regulates paclitaxel resistance via BCL2 and BCLxL, we used cell lines stably expressing wtCAV1, Y14F mutant, or the empty vector (EV). Although both wtCAV1 and Y14F CAV1 localize in mitochondrial fractions, wtCAV1, but not Y14F, readily forms a complex with anti-apoptotic BCL2 and BCLxL. Moreover, expression of wtCAV1, and not Y14F, increases phosphorylation of BCL2 and BCLxL, at Ser-70 and Ser-62, respectively, via JNK, a member of the mitogen-activated protein kinase (MAPK) family. Paclitaxel synergizes with ABT-737, a small molecule inhibitor of BCL2, and restores paclitaxel sensitivity in MCF-7 cells expressing the Y14F mutant. Thus, paclitaxel resistance in these cells occurs primarily through BCL2 and BCLxL activation. Using homology modeling, we show that Tyr-14 phosphorylation of CAV1 results in a structure that enables the CAV1 scaffolding domain (CSD) (9) to be more accessible to bind other proteins. Therefore, in ER^+ breast cancer cells, CAV1 facilitates JNK-mediated phosphorylation/inactivation of BCL2 and BCLxL and enables paclitaxel-induced apoptosis.

EXPERIMENTAL PROCEDURES

Cell Culture and Reagents—MCF-7 human breast cancer cells (obtained from the Lombardi Comprehensive Cancer Center (LCCC) Tissue Culture Shared Resource) were cultured in improved minimal essential medium (Invitrogen) supplemented with 5% fetal bovine serum (FBS) and 1% penicillin/streptomycin. Stable MCF-7 cell lines expressing the empty vector (MCF7/EV), wtCAV1 (MCF7/wtCAV1), or the Y14F CAV1 mutant (MCF7/Y14F) were established and maintained as described previously (18). wtCAV1/CAV1α and CAV1β constructs were a generous gift from Dr. Michael R. Freeman (19), and MCF-7 stable cells expressing wtCAV1/CAV1α, CAV1β or the empty vector (pcDNA3) were made as described previously (18). MCF-7 TaxR30 and MCF-7 TaxR50 and their respective control MCF-7 cells were obtained from Dr. Anthony Letai (Dana-Farber Cancer Institute, Boston, MA); MCF-7 TaxR30 and MCF-7 TaxR50 were maintained in the presence of 30 and 50 nM paclitaxel, respectively, and 5 μg/ml verapamil as described previously (20). Cells were maintained in a humidified atmosphere at 37 °C and 95% air, 5% CO_2. Paclitaxel was obtained from Sigma and was dissolved in ethanol. The inhibitors of JNK (SP600125) and ERK (2′-amino-3′-methoxyflavone (PD98059)) were purchased from EMD (Gibbstown, NJ). ABT-737 was purchased from Selleck Chemicals, Houston, TX). All other reagents were from Sigma unless otherwise indicated.

Western Blot Analyses and Immunoprecipitation—To determine the effects of paclitaxel on CAV1 protein expression, cells were treated with vehicle or 10 nM paclitaxel for 48 h. Controls were treated with vehicle alone (0.02% v/v ethanol). For Western blot analysis, cells were lysed for 30 min at 4 °C in lysis buffer (50 mM Tris-HCl, pH 7.5, containing 150 mM NaCl, 1 mM EDTA, 0.5% sodium deoxycholate, 1% IGEPAL CA-630, 0.1% SDS, 1 mM Na_3VO_4, 44 μg/ml phenylmethylsulfonyl fluoride) supplemented with Complete Mini protease inhibitor mixture tablets (Roche Applied Science). Total protein was quantified using the bicinchoninic acid assay (Pierce). Whole cell lysate (5–50 μg) was resolved by SDS-PAGE. The following primary antibodies were used for immunoblotting: polyclonal antibody against CAV1 (BD Biosciences); phospho-BCL2(Ser-70), COX4, phospho-JNK(Thr-183/Tyr-185), JNK, phospho-c-Jun(Ser-63), BCLxL, and cleaved-PARP (~89 kDa, Cell Signaling, Danvers, MA); BCL2 (StressGen Corp., Ann Arbor, MA); and phospho-BCLxL(Ser-62) (Abcam, Cambridge, MA). Equal protein loading of gels was confirmed by immunostaining with an anti-actin antibody (Santa Cruz Biotechnology, Santa Cruz, CA). For immunoprecipitations with BCL2, BCLxL, or CAV1, lysates were incubated with 1–10 μg/ml primary antibodies for 4 h at 4 °C followed by incubation overnight with protein A/G-agarose beads (eBiosciences, San Diego, CA). For immunoprecipitation with phospho-JNK(Thr-183/Tyr-185), lysates were incubated with antibody-Sepharose bead conjugate (Cell Signaling) at 1 mg/ml overnight. Beads were centrifuged gently and washed with 1× lysis buffer. Bound proteins were resolved by SDS-PAGE as described above.

Subcellular Fractionation—70–80% confluent cells were treated with either vehicle or 10 nM paclitaxel for 48 h. Mitochondria were isolated using with the Qproteome mitochondria isolation kit (Qiagen, Valencia, CA) by following the manufacturer's protocol to isolate cytosolic and mitochondrial fractions. Equal amounts of protein from samples were subjected to Western blotting.

Cell Viability and Apoptosis Assays—To measure cell viability, cells were plated in 96-well plastic tissue culture plates at a density of 5×10^3 cells/well. 24 h after plating, cells were treated with paclitaxel or inhibitors of JNK (SP600125), ERK (PD98059), or BCL2 proteins (ABT-737). After treatment (48 h), cell culture media were removed, and plates were stained with 100 ml/well of a solution containing 0.5% crystal violet and 25% methanol, rinsed with deionized water, dried overnight, and resuspended in 100 ml of citrate buffer (0.1 M sodium citrate in 50% ethanol) to assess plating efficiency. Intensity of crystal violet staining, assessed at 570 nm and quantified using a VMax kinetic microplate reader and SoftMax software (Molecular Devices Corp., Menlo Park, CA), is directly proportional to cell number (21). Data were normalized to vehicle-

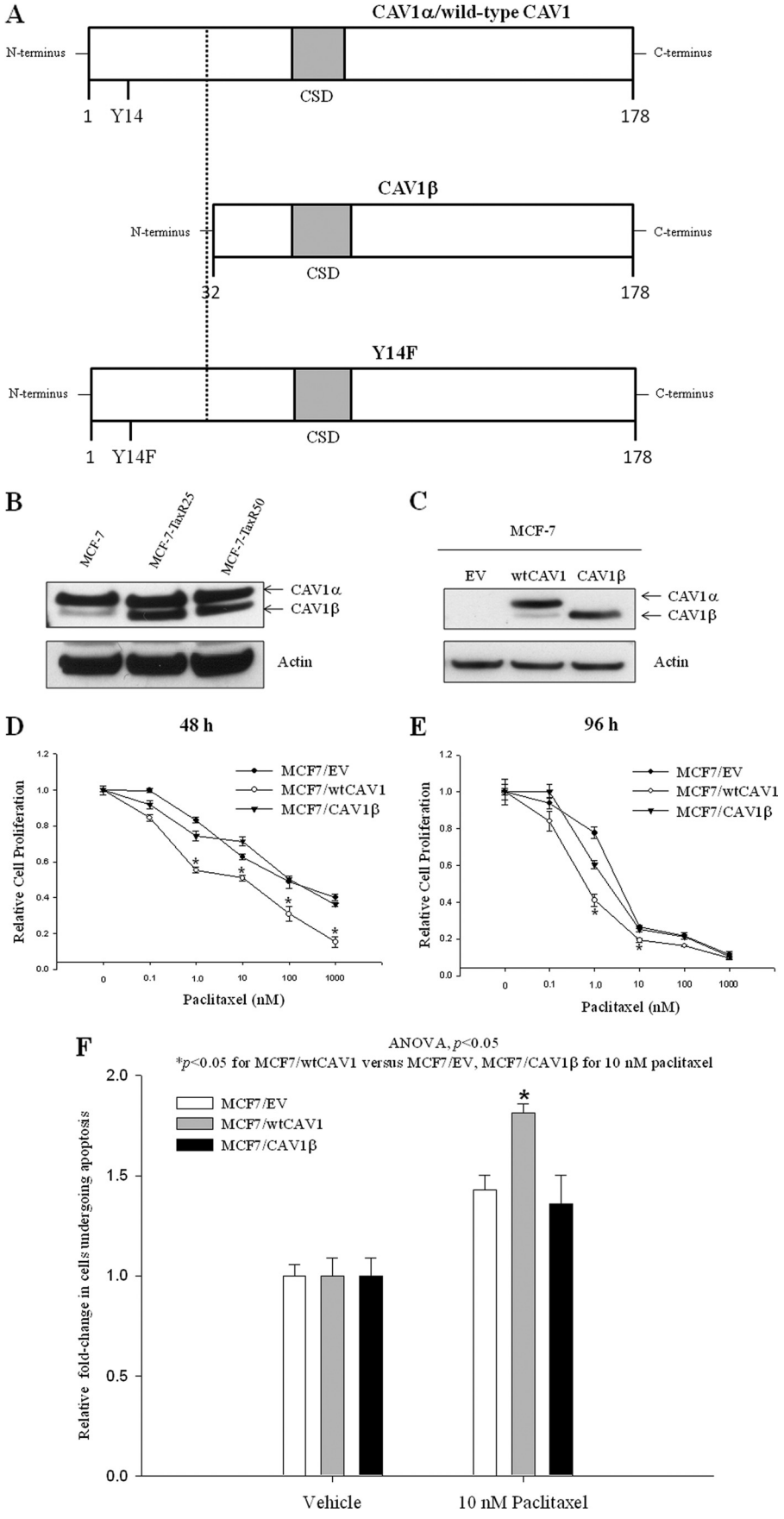
A
CAV1α/wild-type CAV1
N-terminus
C-terminus
CSD
1
Y14
178
CAV1β
32
Y14F
B
MCF-7
MCF-7-TaxR25
MCF-7-TaxR50
CAV1α
CAV1β
Actin
C
MCF-7
EV
wtCAV1
CAV1β
D
48 h
Relative Cell Proliferation
MCF7/EV
MCF7/wtCAV1
MCF7/CAV1β
Paclitaxel (nM)
E
96 h
F
ANOVA, p<0.05
*p<0.05 for MCF7/wtCAV1 versus MCF7/EV, MCF7/CAV1β for 10 nM paclitaxel
Relative fold-change in cells undergoing apoptosis
Vehicle
10 nM Paclitaxel

treated cells and are presented as the mean ± S.E. from representative experiments. To measure apoptosis, cells were treated with 10 nM paclitaxel for 24 h, and annexin V and propidium iodide staining was done using an annexin V-fluorescein isothiocyanate kit (Trevigen, Gaithersburg, MD) and measured by fluorescence-activated cell sorting in the Lombardi Comprehensive Cancer Center Flow Cytometry Shared Resource facility.

Immunostaining and Confocal Microscopy—Cells were grown on coverslips for 24 h and then incubated with 50 μl/ml of medium with CellLight™ mitochondria-RFP (Invitrogen) for an additional 24 h. Cells were then fixed, permeabilized, and incubated with primary antibody for CAV1. Fluorophore conjugates and 4′,6-diamidino-2-phenylindole dihydrochloride (DAPI) were obtained from Molecular Probes, Inc. (Eugene, OR). DAPI was added to visualize nuclei, and nonconfocal DAPI images were acquired using mercury lamp excitation and a UV filter set. Confocal microscopy was performed using an Olympus FV300 confocal microscope with 405-, 488-, and 543-nm excitation lasers. Fluorescence emission was separately detected for each fluorophore in <1-μm-thick optical sections (pinhole set to achieve 1 Airy unit) (22).

Transfection of Small Interfering (si) RNA—Cells were plated in 6-well plates in complete medium and allowed to grow to 60–80% confluence. ~100 nM JNK siRNA (Cell Signaling) or the respective control siRNA was transfected using the TransIT-siQUEST transfection reagent according to the manufacturer's protocol (Mirus, Madison, WI). At 24 h after transfection, 10 nM paclitaxel or vehicle was added to the siRNA transfected cells. At 48 h after treatment, cells were subjected to Western blot analysis as described above to validate protein expression.

Structure Prediction and Molecular Dynamics Simulations—Structural models of CAV1 (wtCAV1, phosphorylated CAV1, or phosphorylated Tyr-14 (Y14p) or Y14F mutant) were built based primarily on the homology-modeled structure of CAV1. Structure of the CAV1 sequence 1–78 was predicted using the x-ray crystal structure of cytochrome *c* oxidase (Protein Data base Bank ID: 1M56) as a template (31% homology). Predicted structural models were energy-minimized using the consistent valence force field (CFF91) with AMBER 9.0 (23). The cutoff for nonbonded interaction energies was set to ∞ (no cutoff); other parameters were set to default. Energy-minimized structures of pCAV1 and Y14F were subjected to 1-ns molecular dynamics simulations conducted with a distance-dependent dielectric constant using the SANDER module of the AMBER 9.0 software (23) and the PARM98 force-field parameter. The SHAKE algorithm (24) was used to keep rigid all bonds involving hydrogen atoms. Weak coupling temperature and pressure coupling algorithms were used to maintain constant temperature and pressure, respectively (25). Molecular dynamics simulations were performed using 0.003-ps time intervals with the temperature set to 300 K. Electrostatic interactions were calculated using the Ewald particle mesh method (26) with a dielectric constant at $1R_{ij}$ and a nonbonded cutoff of 14 Å for the electrostatic interactions and for van der Waals interactions. Structural analyses were done using the SYBYL 8.2 molecular modeling program (Tripos International, St. Louis, MO).

Statistical Analyses—Statistical analyses were performed using the SigmaStat software package (Jandel Scientific, SPSS, Chicago, IL). Where appropriate, protein expression and cell growth were compared using Student's *t* test. Differences were considered significant at $p \leq 0.05$. One-way analysis of variance was used to determine overall significant differences following treatment in apoptosis assays. The interaction between paclitaxel and ABT-737 was evaluated by determining the *R* index (27). *R* index values were obtained by calculating the expected cell survival (S_{exp}; the product of survival obtained with drug A alone and the survival obtained with drug B alone) and dividing S_{exp} by the observed cell survival in the presence of both drugs (S_{obs}). $S_{exp}/S_{obs} > 1.0$ indicates a synergistic interaction (27).

RESULTS

CAV1β Expression Confers Resistance to Paclitaxel in MCF-7 Cells—Breast cancer cells with a weak invasive phenotype, such as MCF-7, express low but detectable levels of CAV1. ~50 μg of total protein was needed to detect endogenous CAV1 expression in nontransfected MCF-7 cells by Western blotting (Fig. 1*B*), whereas 20 μg of total protein was sufficient to detect overexpressed CAV1 (wtCAV1, CAV1β) (Fig. 2*B*). Thus, endogenous levels of CAV1 in Fig. 1*B* are not comparable with those for MCF7/EV cells in Fig. 1*C*. To determine whether the expression levels of CAV1 variants vary in sensitive *versus* resistant breast cancer cells, we compared the expression levels of total CAV1 protein in MCF-7 cells that are either sensitive or resistant to 25 or 50 nM paclitaxel (20). Although CAV1α levels did not change across cell lines, CAV1β levels were increased in the resistant cells when compared with those in sensitive cells (Fig. 1*B*). To test whether responsiveness to paclitaxel in MCF-7 cells differs based on expression of CAV1 variants, stable cell lines expressing wtCAV1, CAV1β, or EV were treated with increasing concentrations of paclitaxel. Fig. 1*C* shows that although MCF7/wtCAV1 cells express both wtCAV1 (or CAV1α) and CAV1β, MCF7/CAV1β cells primarily express CAV1β. MCF7/CAVα cells showed increased sensitivity to paclitaxel when compared with MCF7/CAV1β or MCF7/EV at 48 (Fig. 1*D*) and 96 h (Fig. 1*E*). At 48 h, significantly more

FIGURE 1. **Schematic representation of wtCAV1 or CAV1α, CAV1β, and Y14F mutant.** *A*, the three different constructs of CAV1 used in this study are represented here as bar diagrams: wtCAV1/CAV1α (1–178 amino acids), CAV1β (32–178 amino acids), and the Y14F mutant with Tyr-14 → Phe to denote a single point mutation. The *shaded gray area* is the CSD (80–101 amino acids). The *dashed line* highlights the differences between wtCAV1 and the CAV1β variant. *B*, resistant MCF-7 cells, TaxR25 and TaxR50, express higher levels of CAV1β when compared with their respective paclitaxel-sensitive MCF-7 control cells (20). CAV1 antibody was used to detect the two variants that are easily differentiated by size. *C*, total cell lysates from stable MCF-7 cell lines expressing CAV1α, CAV1β, or the EV (pcDNA3). Note: Basal CAV1 expression in MCF-7 cells is low, and therefore, ~50 μg of protein is used in the blot shown in *A*, whereas 20 μg of protein is used in the blot shown in *C*. *D* and *E*, relative cell proliferation in MCF7/EV, MCF7/CAV1α, or MCF7/CAV1β was measured in response to increasing concentrations of paclitaxel for 48 (*D*) and 96 h (*E*). Inhibition of cell proliferation by increasing doses of paclitaxel was significantly increased in MCF7/CAV1α cells when compared with MCF7/EV or MCF7/CAV1β cells. *, $p \leq 0.001$ *versus* MCF7/EV or MCF7/CAV1β at 1, 10, 100, and 1000 nM paclitaxel for 48 h and at 1 and 10 nM paclitaxel for 96 h by Student's *t* test. *F*, apoptosis in MCF7/wtCAV1 cells was significantly increased when compared with MC7/EV or MCF7/CAV1β cells within 24 h following 10 nM paclitaxel treatment. ANOVA, analysis of variance.

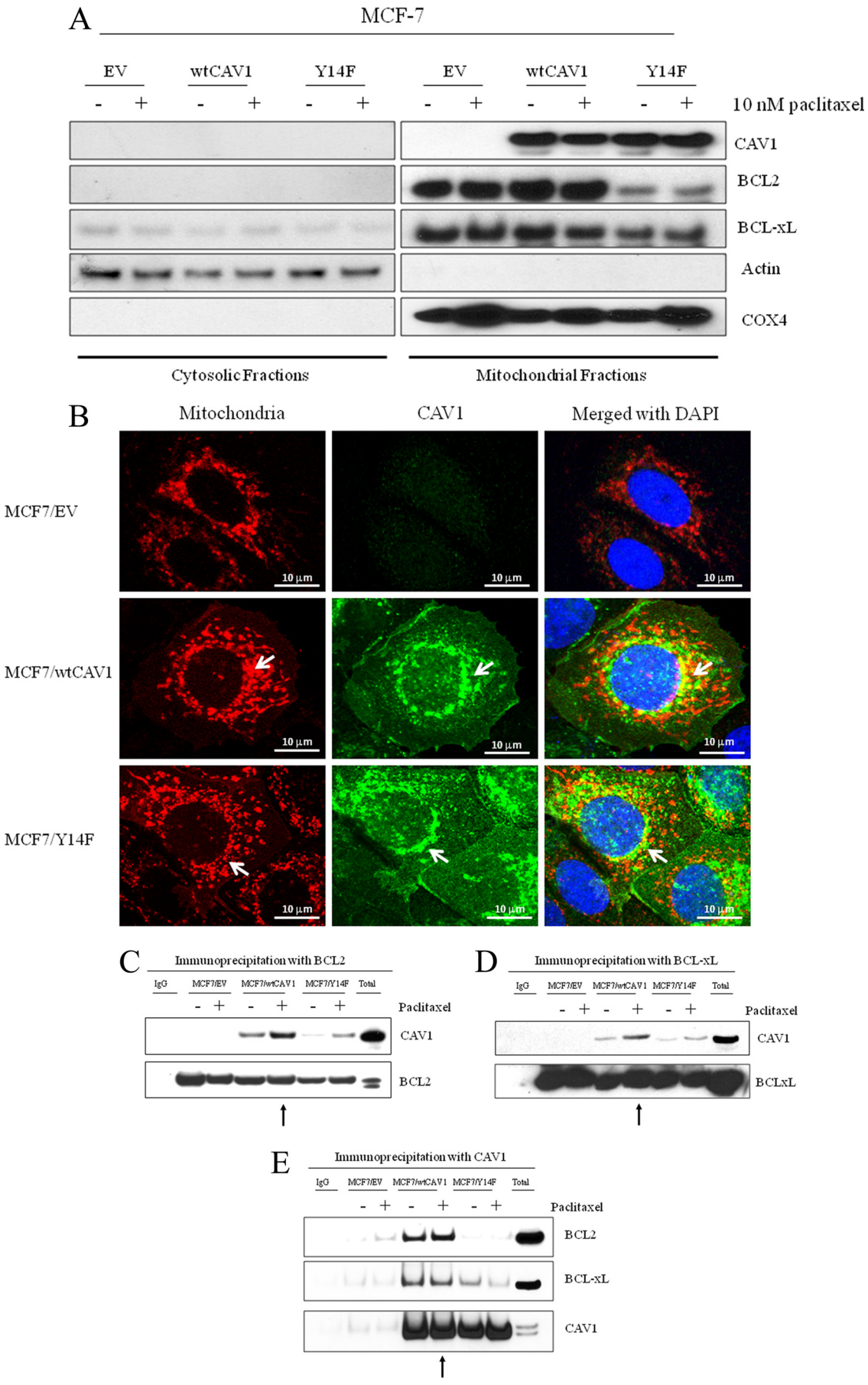
A
MCF-7
EV
wtCAV1
Y14F
EV
wtCAV1
Y14F
- + - + - + - + - + - +
10 nM paclitaxel
CAV1
BCL2
BCL-xL
Actin
COX4
Cytosolic Fractions
Mitochondrial Fractions
B
Mitochondria
CAV1
Merged with DAPI
MCF7/EV
MCF7/wtCAV1
MCF7/Y14F
10 μm
C
Immunoprecipitation with BCL2
IgG
MCF7/EV
MCF7/wtCAV1
MCF7/Y14F
Total
- + - + - +
Paclitaxel
CAV1
BCL2
D
Immunoprecipitation with BCL-xL
IgG
MCF7/EV
MCF7/wtCAV1
MCF7/Y14F
Total
- + - + - +
Paclitaxel
CAV1
BCLxL
E
Immunoprecipitation with CAV1
IgG
MCF7/EV
MCF7/wtCAV1
MCF7/Y14F
Total
- + - + - +
Paclitaxel
BCL2
BCL-xL
CAV1

MCF7/wtCAV1 cells undergo apoptosis following treatment with 10 nM paclitaxel when compared with MCF7/EV or MCF7/CAV1β cells (Fig. 1*F*). Thus, signaling that is regulated by the 31 amino acids of wtCAV1, which are absent in CAV1β, is important in determining paclitaxel-mediated inhibition of cell survival.

CAV1 Localizes to Mitochondria and Forms Complexes with BCL2 and BCLxL That Are Dependent upon Tyr-14 Phosphorylation—Fractionation of mitochondrial and cytosolic fractions were carried out in stably transfected MCF-7 cells that express the empty vector (MCF7/EV), wild-type CAV1 (MCF7/wtCAV1), or a tyrosine phosphorylation-deficient mutant (MCF7/Y14F) (18). Each cell line was treated with either vehicle (ethanol) or 10 nM paclitaxel for 48 h. Western blot analyses of fractionated proteins showed the presence of both wtCAV1 and Y14F in the mitochondria irrespective of drug treatment (Fig. 3*A*). Moreover, both wtCAV1 and the Y14F mutant partly co-localized with a mitochondrion-specific fluorescent reagent (see under "Experimental Procedures": CellLight™ mitochondria-RFP) (Fig. 2*B*). Primarily, CAV1 co-localized with a subset of mitochondria surrounding the nucleus. CAV1 staining was also present in other areas of the cell that did not stain with the mitochondrion-specific dye. Therefore, CAV1 is also present in nonmitochondrial compartments. Thus, phosphorylation on Tyr-14 does not control localization of CAV1 to the mitochondria. Because overexpression of wtCAV1 increased BCL2 phosphorylation and mitochondrial permeability following paclitaxel treatment (18), we explored the possible interaction between CAV1 and BCL2 or BCLxL. Whole cell lysates from MCF7/EV, MCF7/wtCAV1, or MCF7/Y14F cells were immunoprecipitated using antibodies specific for BCL2 or BCLxL followed by immunoblotting with a CAV1 antibody. Increased amounts of wtCAV1 immunoprecipitated with both BCL2 and BCLxL when compared with the Y14F mutant form following treatment with 10 nM paclitaxel for 24 h (Fig. 2,*C* and *D*). Similarly, when whole cell lysates were immunoprecipitated with a CAV1 antibody (Fig. 2*E*), increased amounts of BCL2 and BCLxL immunoprecipitated with wtCAV1 when compared with Y14F. Thus, phosphorylation on Tyr-14 may facilitate CAV1 complex formation with BCL2 and BCLxL.

wtCAV1 Expression Potentiates BCL2(Ser-70) and BCLx-L(Ser-62) Phosphorylation by JNK—In MCF7/wtCAV1 cells, the level of phosphorylated BCL2(Ser-70) detected following 24 h of treatment with 10 nM paclitaxel is significantly higher than in either control or MCF7/Y14F cells (18). Mitogen-activated protein (MAP) kinase pathways such as JNK, ERK, and p38 are activated by paclitaxel and may regulate BCL2(Ser-70) phosphorylation (28–31). To determine whether CAV1 regulates the aforementioned MAP kinase pathways to control BCL2 and BCLxL activation, we measured their activation in cells treated with either vehicle or 10 nM paclitaxel. Although no significant differences were seen for ERK or p38 (data not shown), increased JNK phosphorylation was detected in MCF7/wtCAV1 cells when compared with MCF7/Y14F or MCF7/EV cells (Fig. 3*A*). Consequently, immunoprecipitation with phospho-JNK-conjugated Sepharose beads from whole cell lysates from MCF7/EV, MCF7/wtCAV1, and MCF7/Y14F showed increased levels of wtCAV1 bound to phospho-JNK with either vehicle or 10 nM paclitaxel treatment (Fig. 3*B*). Thus, CAV1 phosphorylation on Tyr-14 may favor complex formation with JNK. To test this, we measured cell viability in the presence of paclitaxel and a specific inhibitor of JNK (10 μM, SP600125). Inhibition of JNK decreased paclitaxel-mediated inhibition of cell viability (Fig. 3*C*) and apoptosis as indicated by PARP cleavage (Fig. 3*D*) in MCF7/wtCAV1 cells. In addition, inhibition of JNK with the JNK-specific inhibitor SP600125 abolished BCL2 and BCLxL phosphorylation at Ser-70 and Ser-62, respectively, in MCF7/wtCAV1 cells (Fig. 3*E*). A specific antibody to phosphorylated c-Jun(Ser-63), a substrate for JNK (32), was used to detect activation of JNK. Knockdown of JNK with specific siRNA inhibited paclitaxel-induced phosphorylation of BCL2(Ser-70) and BCLxL(Ser-62) in MCF7/wtCAV1 cells (Fig. 3*F*). Thus, CAV1 phosphorylation on Tyr-14 may favor activation of JNK and its consequent phosphorylation of BCL2 and BCLxL.

ABT-737 Synergistically Increases Sensitivity to Paclitaxel in MCF-7/Y14F Cells—Because overexpression of wtCAV1 in MCF-7 cells phosphorylates and thereby inhibits BCL2 and BCLxL activity to sensitize cells to paclitaxel, inhibition of BCL2 and BCLxL in the resistant MCF7/Y14F cells may restore sensitivity to paclitaxel. MCF7/EV, MCF7/wtCAV1, and MCF7/Y14F cells were treated with the small molecule BCL2 inhibitor ABT-737, a BH3-only mimetic that disrupt the anti-apoptotic functions of BCL2, BCLxL, and BCLW by binding to their hydrophobic cleft (33). MCF7/Y14F cells were most sensitive to increasing doses of ABT-737 (Fig. 4*A*) when compared with either MCF7/wtCAV1 or MCF7/EV cells. Furthermore, although 100 nM ABT-737 was ineffective in further sensitizing MCF7/EV or MCF7/wtCAV1 cells to 10 nM paclitaxel, it synergistically increased inhibition of cell viability as indicated by *R* index = 2.48 (see "Statistical Analyses") in MCF7/Y14F cells (Fig. 4*B*). An increase in PARP cleavage was also apparent in MCF7/Y14F cells following treatment with paclitaxel and ABT-737 *versus* paclitaxel alone (Fig. 4*C*).

Structural Modeling of CAV1 and Y14p and Y14F Mutants—The crystal structure of CAV1 protein remains to be determined. However, using *in silico* structural modeling, we obtained key

FIGURE 2. **CAV1 is localized in mitochondria in MCF-7 breast cancer cells, and BCL2 and BCLxL preferentially complex with wtCAV1.** *A*, immunoblot showing mitochondrial and cytoplasmic fractions of MCF7/EV, MCF7/wtCAV1, and MCF7/Y14F cells following treatment with 10 nM paclitaxel for 24 h. Actin and COX4 were used as cytosolic and mitochondrial markers, respectively. Both wtCAV1 and Y14F were found in mitochondrial fractions. *B*, merged confocal images showing mitochondria stained *red* with CellLight™ mitochondria-RFP (Invitrogen), CAV1 in *green*, nuclei in *blue* (DAPI) in MCF7/EV, MCF7/wtCAV1, and MCF7/Y14F cells under basal conditions. Co-localization of CAV1 with mitochondria are in *yellow*. Very low levels of CAV1 were detected in EV-expressing cells when compared with wtCAV1- or Y14F-expressing cells. Note that not all CAV1 co-localized with mitochondria. *Scale bar*, 10 μm. *C*, *D*, and *E*, co-immunoprecipitation of BCL2 or BCLxL with CAV1 is increased in MCF7/wtCAV1 cells. MCF7/EV, MCF7/wtCAV1, or MCF7/Y14F were treated with 10 nM paclitaxel for 24 h. Total cell lysates were immunoprecipitated using either BCL2 or BCLxL antibodies, and bound proteins were immunoblotted with CAV, BLC2, or BCLxL antibodies. *Arrows* point toward total CAV1 precipitated in MCF7/wtCAV1 cells following paclitaxel treatment.

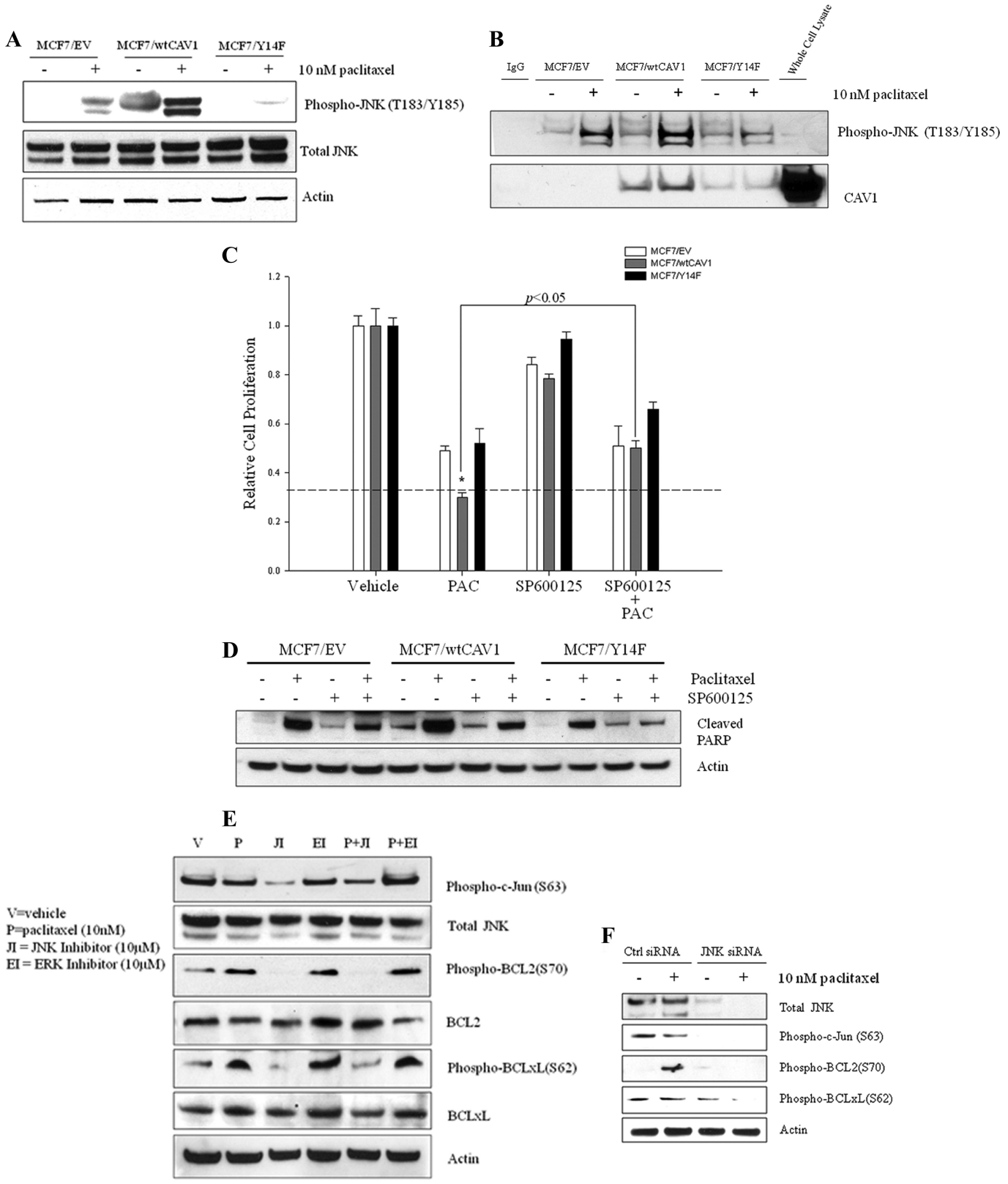

FIGURE 3. **Regulation of BCL2/BCLxL phosphorylation by JNK determines sensitivity to paclitaxel in MCF7/wtCAV1 cells.** *A*, JNK phosphorylation is increased in MCF-7/wtCAV1 cells. *B*, immunoprecipitation of phospho-JNK(Thr-183/Thr-185)-conjugated Sepharose beads in MCF7/EV, MCF7/wtCAV1, and MCF7/Y14F cells was carried out following treatment with vehicle alone or 10 nM paclitaxel to determine whether active JNK forms complexes with CAV1. Increased phosphorylation of JNK in MCF7/wtCAV1 (see *A*) correlated with increased complex formation with wtCAV1 in cells treated with either vehicle or 10 nM paclitaxel treatment for 24 h (see *B*). Even under basal conditions (vehicle), phospho-JNK(Thr-183/Tyr-185)-conjugated Sepharose beads pulled down more wtCAV1 when compared with Y14F. *C*, activation of JNK is required for paclitaxel-mediated inhibition of cell proliferation in MCF7/wtCAV1 cells. The *dashed line* compares treatment with paclitaxel alone (*PAC*) *versus* paclitaxel plus the inhibitor of JNK, SP600125 (*SP600125 + PAC*). *, $p < 0.05$. *D*, inhibition of JNK greatly decreased cleavage of PARP (indicative of apoptosis) in MCF7/wtCAV1 cells. *E*, inhibition of JNK with SP600125. *F*, knockdown of JNK with siRNA abolished phosphorylation of BCL2 and BCLxL.

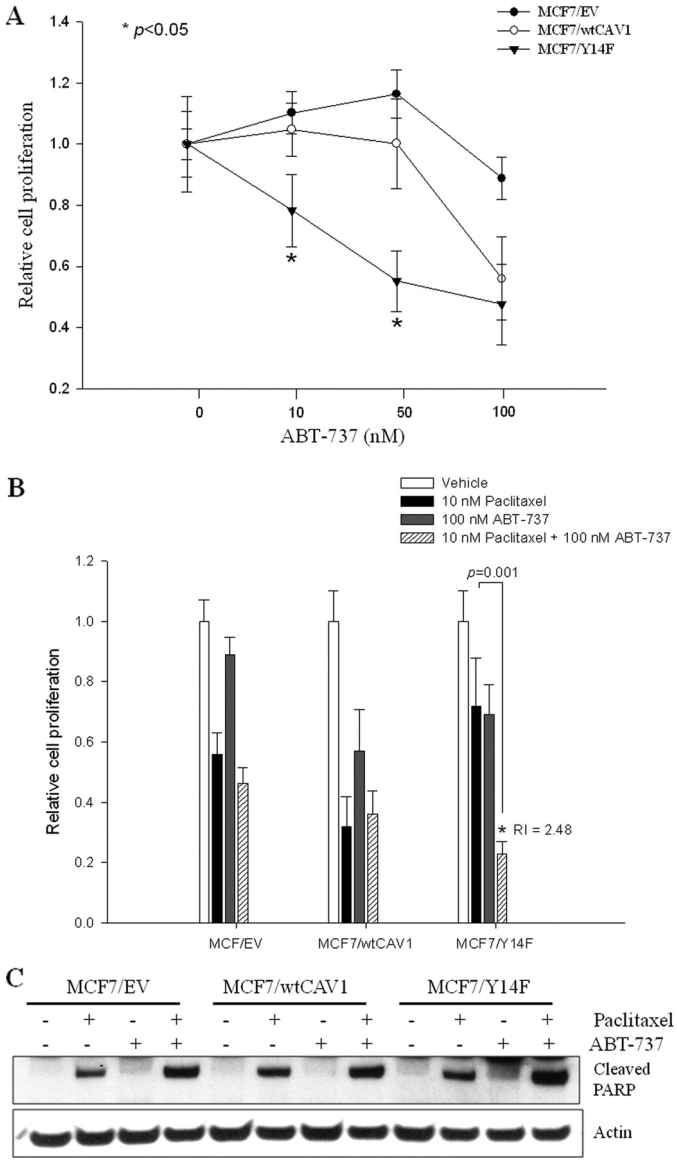

FIGURE 4. **ABT-737 reverses Y14F-mediated protection of MCF-7 cells from paclitaxel-induced inhibition of cell proliferation.** *A*, cell proliferation was measured in MCF7/EV, MCF7/wtCAV1, and MCF7/Y14F cells in response to different doses of ABT-737 for 48 h. MCF7/Y14F cells showed increased sensitivity to 10 and 50 nM ABT-737 when compared with MCF7/EV or MCF7/wtCAV1 cells. *, $p < 0.05$ for MCF7/Y14F *versus* MCF7/EV or MCF7/wtCAV1 cells by Student's *t* test. *B*, MCF7/EV, MCF7/wtCAV1, and MCF7/Y14F cells were treated with vehicle, 10 nM paclitaxel, 100 nM ABT-737, or the combination of 10 nM paclitaxel and 100 nM ABT-737 for 48 h. In MCF7/Y14F cells, the combination synergistically inhibited cell proliferation. *Bars* represent the mean of three independent experiments ± S.E. *, $p < 0.05$, 10 nM paclitaxel and 100 nM ABT-737 when compared with paclitaxel only by Student's *t* test. *R* index (*RI*) = 2.48 indicates synergy (see under "Experimental Procedures" for statistical analysis). *C*, level of cleaved PARP (indicative of apoptosis) was increased in MCF7/Y14F cells that were co-treated with ABT-737 and paclitaxel when compared with levels in MCF7/Y14F cells treated with paclitaxel alone.

insights into the likely biological roles of Tyr-14. We modeled CAV1 (amino acid 6–85) as a phosphorylated Tyr-14 (Y14p) in wtCAV1 and as the Y14F mutant protein (as described under "Experimental Procedures"). In wtCAV1, Tyr-14 forms a network of hydrogen bonds with the adjacent charged residues at His-12 and Glu-20 (Fig. 5*A*). Phosphorylation at Tyr-14 (Y14p) introduces a negatively charged moiety that disrupts the interaction of Tyr-14 with His-12 and Glu-20. The His-12 residue forms a salt bridge with the phosphate group of Tyr-14 and a hydrogen bond interaction with Glu-20 (Fig. 5*A*). Because of the high net negative charge of the phosphate group, Glu-20 is predicted to move away from, and the positively charged Arg-19 moves toward, the negatively charged phosphate group to form a salt bridge. His-12 and Glu-10 contribute to maintaining stability of the salt bridge. Consequently, when phosphorylated, Tyr-14 enables the N-terminal region of CAV1 to fold into a more compact structure. This folding likely reorients the nearby CSD to create an interface that favors the interaction with other proteins containing CAV1-binding motifs (*e.g.* Φ*XXXX*Φ*XX*Φ) (34). Unlike wCAV1, Y14F is predicted to exhibit unfavorable hydrophobic properties in the exposed surface. Consequently, the CSD is pushed inward and excluded from the protein surface (Fig. 5*B*). This movement of Y14F affects the neighboring residues, and in turn, alters the local folding. For example, Gln-21 now replaces Y14F at the interface to compensate for the hydrophobicity of Y14F (Fig. 5*B*). Glu-20 and Arg-19 are also refolded to make the salt bridge. Thus, the presence of Phe at Tyr-14 changes CAV1 folding, is expected to alter the interface shape and size, and modifies the net charge on the surface.

DISCUSSION

Response rates to paclitaxel vary widely among breast cancer patients (4); to date, there are no predictive molecular markers for paclitaxel sensitivity. Our group was the first to show that phosphorylated CAV1 triggers paclitaxel-mediated apoptosis by inactivating BCL2 and increasing mitochondrial permeability more efficiently than nonphosphorylated CAV1 (18). Although the role of CAV1 phosphorylation in paclitaxel responsiveness remains unknown, sustained phosphorylation of CAV1 and BCL2 occurs upon paclitaxel treatment in HeLa cells (35). The data presented here uniquely show that expression of wtCAV1/CAV1α, which harbors the Tyr-14 residue, sensitizes ER^+ breast cancer cells to paclitaxel by inhibiting BCL2 and BCLxL. Moreover, paclitaxel-resistant MCF-7 cells up-regulate expression levels of CAV1β when compared with sensitive cells. Increased levels of both wtCAV1 and Y14F CAV1 were present in mitochondrial fractions from MCF-7 cells before and after paclitaxel treatment, but wtCAV1 formed more complexes with BCL2 and BCLxL. The precise function of CAV1 in the mitochondria remains unknown, but our data show that phosphorylated CAV1 (on Tyr-14) increases its interaction with BCL2 and BCLxL. Thus, wtCAV1 may facilitate cell death by sequestering specific signaling molecules involved in apoptosis. To date, the specific role of CAV1 variants has remained unclear. CAV1 variant-dependent sequestration of essential apoptotic regulators such as BCL2 and BCLxL may explain why paclitaxel-resistant breast cancer cells overexpress CAV1β to evade apoptosis.

MAPK family members such as ERK (36), p38 (37), and JNK (38) can become activated following paclitaxel treatment. Although activation of ERK1 and p38 protects cells from the cytotoxic affects of paclitaxel, activation of JNK is associated with increased sensitivity to paclitaxel (39). Paclitaxel causes a rapid increase in JNK activation, and inhibition of JNK is associated with decreased levels of paclitaxel-mediated apoptosis (40). Induction of JNK activation following paclitaxel treatment

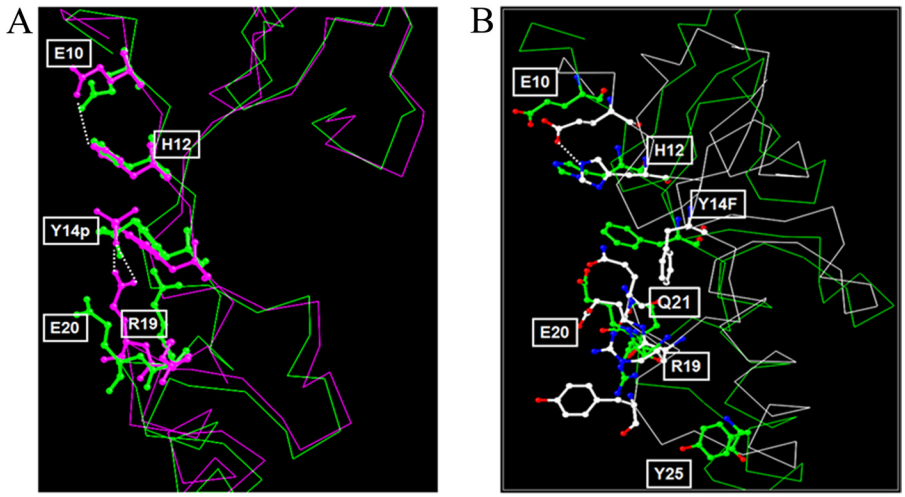

FIGURE 5. **Structural modeling of CAV1-phosphorylated Tyr-14 *versus* Y14F mutant.** *A*, the conformation corresponding to the initial state of the phosphorylated Tyr-14 CAV1 (Y14p) (*green*) superimposed with the final state (*magenta*) after a 1-ns simulation. *B*, the conformation corresponding to initial state of the Y14F mutant (*green*) superimposed with the final state (*white*) after a 1-ns simulation. In both cases, *broken lines* indicate hydrogen bonds.

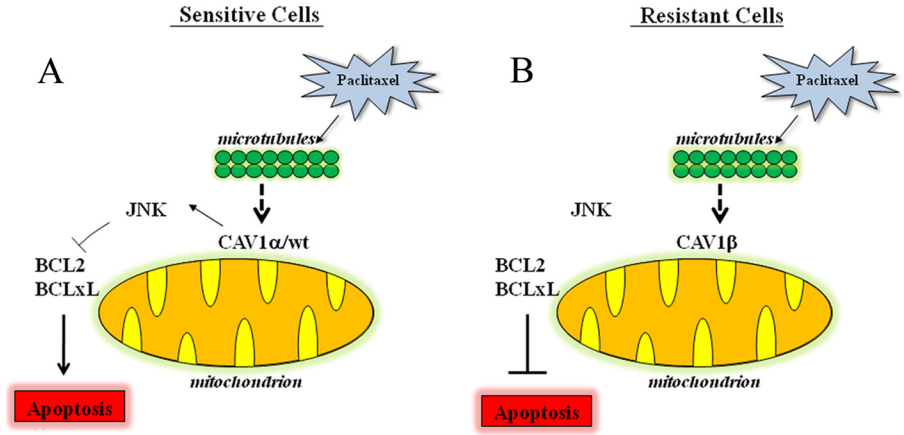

FIGURE 6. **Simplified model of CAV1 regulation of paclitaxel sensitivity.** *A*, in sensitive cells, upon treatment with paclitaxel, wtCAV forms a complex with JNK and thereby leads to inactivation of BCL2 and BCLxL, which facilitates apoptosis. *B*, in resistant cells, where CAV1β is predominant, CAV1β does not associate with JNK and BCL2, and BCLxL remains active to inhibit apoptosis.

may be a converging point for both drug-induced apoptosis and activation of genes such as interleukin-8 (IL-8) that may indirectly facilitate cell death (38). Modulation of MAPK signaling, in response to cytotoxic drugs, depends on cellular context and can either enhance or decrease drug activity (41). Because MAPKs can interact with the CAV1 CSD (34), CAV1-JNK complex formation may regulate the activation/function of JNK following paclitaxel treatment.

Alterations in the intrinsic apoptotic pathway, which is regulated by pro-survival BCL2 family members, could contribute to paclitaxel resistance. Combining small molecule BCL2 antagonists such as ATB-737 with paclitaxel could resensitize breast cancer cells to this taxane (20). Phosphorylation of BCL2 (28, 30, 42) and BCLxL (29) by the stress-activated kinase JNK can inhibit their pro-survival function. Increased BCL2 phosphorylation corresponds to increased sensitivity to paclitaxel in MCF-7 cells (18). We now show that JNK activation is greatest in MCF7/wtCAV1 cells. MCF7/wtCAV1 cells express increased level of phospho-JNK and show increased binding of wtCAV1 with vehicle or paclitaxel treatment (Fig. 3*B*). Thus, wtCAV1 may help sequester phospho-JNK along with BCL2 and BCLxL, and thereby, may inhibit BLC2 and BCLxL more efficiently than the Y14F mutant.

Emerging data suggest an essential, but yet unclear, role for BCL2 in paclitaxel-mediated cell death. Up-regulation of BCL2 is associated with better clinical outcome and favorable prognosis for some cancers (43). In human ovarian cancer cell lines and tumors, down-regulation of BCL2 correlated with increased resistance to paclitaxel (44). BCL2 levels in human hepatoblastoma HepG2 cells did not affect sensitivity, whereas down-regulation of BCLxL increased sensitivity to paclitaxel (45). Factors that regulate expression levels of BCL2 or BCLxL in human cancers remain unknown. Whether CAV1 variants regulate BCL2 and/or BCLxL transcription is yet to be determined.

Phosphorylated proteins can form docking scaffolds that enable the assembly of other proteins into a functional complex (46). Homology modeling of CAV1 suggests that the aromatic ring of Tyr-14 forms a stable structure to facilitate protein binding to the scaffolding domain. Tyrosine phosphorylation of CAV1 is an important determinant of caveolae formation (47), and paclitaxel treatment can modulate both CAV1 phosphorylation and caveolae dynamics (35). Within caveolae, CAV1 can

bind to various signaling molecules (6, 7). Thus, paclitaxel-resistant breast cancer cells may increase CAV1β to dismantle signaling complexes that favor paclitaxel-mediated apoptosis. In sensitive cells, wtCAV1 enables the formation of a JNK-BCL2-BCLxL complex to allow apoptosis. In resistant cells, overexpression of CAV1β, which is unable to complex with JNK-BCL2-BCLxL, inhibits apoptosis (Fig. 6). Sensitivity to paclitaxel in ER^+ breast cancer cells is regulated by pro-survival BCL2 proteins (20, 48). Because expression of CAV1β in MCF-7 cells failed to increase sensitivity to paclitaxel, the presence of increased levels of CAV1β in paclitaxel-resistant cells likely competes with the CAV1α to prevent phosphorylation/inactivation of BCL2 and BCLxL via JNK.

Acknowledgments—We thank Dr. Michael Johnson (Georgetown University) for helpful discussions and critical review of this manuscript. Technical services were provided by the Flow Cytometry and Cell Sorting, Tissue Culture Core and Microscopy, and Imaging Shared Resources Center, which were funded through National Institutes of Health Award 1P30-CA-51008 from the USPHS (Lombardi Comprehensive Cancer Center Support Grant).

REFERENCES

1. Henderson, I. C., Berry, D. A., Demetri, G. D., Cirrincione, C. T., Goldstein, L. J., Martino, S., Ingle, J. N., Cooper, M. R., Hayes, D. F., Tkaczuk, K. H., Fleming, G., Holland, J. F., Duggan, D. B., Carpenter, J. T., Frei, E., 3rd, Schilsky, R. L., Wood, W. C., Muss, H. B., and Norton, L. (2003) Improved outcomes from adding sequential Paclitaxel but not from escalating Doxorubicin dose in an adjuvant chemotherapy regimen for patients with node-positive primary breast cancer. *J. Clin. Oncol.* **21,** 976–983
2. Mamounas, E. P., Bryant, J., Lembersky, B., Fehrenbacher, L., Sedlacek, S. M., Fisher, B., Wickerham, D. L., Yothers, G., Soran, A., and Wolmark, N. (2005) Paclitaxel after doxorubicin plus cyclophosphamide as adjuvant chemotherapy for node-positive breast cancer: results from NSABP B-28. *J. Clin. Oncol.* **23,** 3686–3696
3. Paridaens, R., Biganzoli, L., Bruning, P., Klijn, J. G., Gamucci, T., Houston, S., Coleman, R., Schachter, J., Van Vreckem, A., Sylvester, R., Awada, A., Wildiers, J., and Piccart, M. (2000) Paclitaxel versus doxorubicin as first-line single-agent chemotherapy for metastatic breast cancer: a European Organization for Research and Treatment of Cancer Randomized Study with cross-over. *J. Clin. Oncol.* **18,** 724–733
4. McGrogan, B. T., Gilmartin, B., Carney, D. N., and McCann, A. (2008) Taxanes, microtubules, and chemoresistant breast cancer. *Biochim. Biophys. Acta* **1785,** 96–132
5. Danial, N. N., and Korsmeyer, S. J. (2004) Cell death: critical control points. *Cell* **116,** 205–219
6. Burgermeister, E., Liscovitch, M., Röcken, C., Schmid, R. M., and Ebert, M. P. (2008) Caveats of caveolin-1 in cancer progression. *Cancer Lett.* **268,** 187–201
7. Goetz, J. G., Lajoie, P., Wiseman, S. M., and Nabi, I. R. (2008) Caveolin-1 in tumor progression: the good, the bad, and the ugly. *Cancer Metastasis Rev.* **27,** 715–735
8. Scherer, P. E., Tang, Z., Chun, M., Sargiacomo, M., Lodish, H. F., and Lisanti, M. P. (1995) Caveolin isoforms differ in their N-terminal protein sequence and subcellular distribution: identification and epitope mapping of an isoform-specific monoclonal antibody probe. *J. Biol. Chem.* **270,** 16395–16401
9. Li, S., Couet, J., and Lisanti, M. P. (1996) Src tyrosine kinases, Gα subunits, and H-Ras share a common membrane-anchored scaffolding protein, caveolin: caveolin binding negatively regulates the auto-activation of Src tyrosine kinases. *J. Biol. Chem.* **271,** 29182–29190
10. Li, S., Seitz, R., and Lisanti, M. P. (1996) Phosphorylation of caveolin by Src tyrosine kinases: the α-isoform of caveolin is selectively phosphorylated by v-Src *in vivo*. *J. Biol. Chem.* **271,** 3863–3868
11. Liu, P., Li, W. P., Machleidt, T., and Anderson, R. G. (1999) Identification of caveolin-1 in lipoprotein particles secreted by exocrine cells. *Nat. Cell Biol.* **1,** 369–375
12. Machleidt, T., Li, W. P., Liu, P., and Anderson, R. G. (2000) Multiple domains in caveolin-1 control its intracellular traffic. *J. Cell Biol.* **148,** 17–28
13. Quest, A. F., Gutierrez-Pajares, J. L., and Torres, V. A. (2008) Caveolin-1: an ambiguous partner in cell signaling and cancer. *J. Cell Mol. Med.* **12,** 1130–1150
14. Patani, N., Martin, L. A., Reis-Filho, J. S., and Dowsett, M. (2012) The role of caveolin-1 in human breast cancer. *Breast Cancer Res. Treat.* **131,** 1–15
15. Hurlstone, A. F., Reid, G., Reeves, J. R., Fraser, J., Strathdee, G., Rahilly, M., Parkinson, E. K., and Black, D. M. (1999) Analysis of the caveolin-1 gene at human chromosome 7q31.1 in primary tumors and tumor-derived cell lines. *Oncogene* **18,** 1881–1890
16. Savage, K., Lambros, M. B., Robertson, D., Jones, R. L., Jones, C., Mackay, A., James, M., Hornick, J. L., Pereira, E. M., Milanezi, F., Fletcher, C. D., Schmitt, F. C., Ashworth, A., and Reis-Filho, J. S. (2007) Caveolin 1 is overexpressed and amplified in a subset of basal-like and metaplastic breast carcinomas: a morphologic, ultrastructural, immunohistochemical, and *in situ* hybridization analysis. *Clin. Cancer Res.* **13,** 90–101
17. Fang, P. K., Solomon, K. R., Zhuang, L., Qi, M., McKee, M., Freeman, M. R., and Yelick, P. C. (2006) Caveolin-1α and -1β perform nonredundant roles in early vertebrate development. *Am. J. Pathol.* **169,** 2209–2222
18. Shajahan, A. N., Wang, A., Decker, M., Minshall, R. D., Liu, M. C., and Clarke, R. (2007) Caveolin-1 tyrosine phosphorylation enhances paclitaxel-mediated cytotoxicity. *J. Biol. Chem.* **282,** 5934–5943
19. Fang, Y., Yan, J., Ding, L., Liu, Y., Zhu, J., Huang, C., Zhao, H., Lu, Q., Zhang, X., Yang, X., and Ye, Q. (2004) XBP-1 increases ERα transcriptional activity through regulation of large-scale chromatin unfolding. *Biochem. Biophys. Res. Commun.* **323,** 269–274
20. Kutuk, O., and Letai, A. (2008) Alteration of the mitochondrial apoptotic pathway is key to acquired paclitaxel resistance and can be reversed by ABT-737. *Cancer Res.* **68,** 7985–7994
21. Bouker, K. B., Skaar, T. C., Fernandez, D. R., O'Brien, K. A., Riggins, R. B., Cao, D., and Clarke, R. (2004) Interferon regulatory factor-1 mediates the proapoptotic but not cell cycle arrest effects of the steroidal anti-estrogen ICI 182,780 (Faslodex, Fulvestrant). *Cancer Res.* **64,** 4030–4039
22. Shajahan, A. N., Timblin, B. K., Sandoval, R., Tiruppathi, C., Malik, A. B., and Minshall, R. D. (2004) Role of Src-induced dynamin-2 phosphorylation in caveolae-mediated endocytosis in endothelial cells. *J. Biol. Chem.* **279,** 20392–20400
23. Case, D. A., Darden, T. A., Cheatham, T. E., Simmerling, C. L., Wang, J., Duke, R. E., Luo, R., Merz, K. M., Pearlman, D. A., Crowley, M., Walker, R. C., Zhang, W., Wang, B., Hayik, S., Roitberg, A., Seabra, G., Wong, K. F., Paesani, F., Wu, X., Brozell, S., Tsui, V., Gohlke, H., Yang, L., Tan, C., Mongan, J., Hornak, V., Cui, G., Beroza, P., Mathews, D. H., Schafmeister, C., Ross, W. S., Kollman, P. A., and (2006) *AMBER 9*, University of California, San Francisco, CA
24. Hanson, R. N., Lee, C. Y., Friel, C. J., Dilis, R., Hughes, A., and DeSombre, E. R. (2003) Synthesis and evaluation of 17α-20E-21-(4-substituted phenyl)-19-norpregna-1,3,5(10),20-tetraene-3,17β-diols as probes for the estrogen receptor α hormone binding domain. *J. Med. Chem.* **46,** 2865–2876
25. Berendsen, H. J. C., Postma, J. P. M., Vangunsteren, W. F., Dinola, A., and Haak, J. R. (1984) Molecular dynamics with coupling to an external bath. *J. Chem. Phys.* **81,** 3684–3690
26. Darden, T., York, D., and Pedersen, L. (1993) Particle mesh Ewald: an *N*.Log(*N*) method for Ewald sums in large systems. *J. Chem. Phys.* **98,** 10089–10092
27. Romanelli, S., Perego, P., Pratesi, G., Carenini, N., Tortoreto, M., and Zunino, F. (1998) *In vitro* and *in vivo* interaction between cisplatin and topotecan in ovarian carcinoma systems. *Cancer Chemother. Pharmacol.* **41,** 385–390
28. Basu, A., You, S. A., and Haldar, S. (2000) Regulation of Bcl2 phosphorylation by stress response kinase pathway. *Int. J. Oncol.* **16,** 497–500
29. Basu, A., and Haldar, S. (2003) Identification of a novel Bcl-xL phospho-

rylation site regulating the sensitivity of taxol- or 2-methoxyestradiol-induced apoptosis. *FEBS Lett.* **538,** 41–47
30. Basu, A., DuBois, G., and Haldar, S. (2006) Posttranslational modifications of Bcl2 family members: a potential therapeutic target for human malignancy. *Front Biosci.* **11,** 1508–1521
31. Yamamoto, K., Ichijo, H., and Korsmeyer, S. J. (1999) BCL-2 is phosphorylated and inactivated by an ASK1/Jun N-terminal protein kinase pathway normally activated at G_2/M. *Mol. Cell Biol.* **19,** 8469–8478
32. Davis, R. J. (2000) Signal transduction by the JNK group of MAP kinases. *Cell* **103,** 239–252
33. Oltersdorf, T., Elmore, S. W., Shoemaker, A. R., Armstrong, R. C., Augeri, D. J., Belli, B. A., Bruncko, M., Deckwerth, T. L., Dinges, J., Hajduk, P. J., Joseph, M. K., Kitada, S., Korsmeyer, S. J., Kunzer, A. R., Letai, A., Li, C., Mitten, M. J., Nettesheim, D. G., Ng, S., Nimmer, P. M., O'Connor, J. M., Oleksijew, A., Petros, A. M., Reed, J. C., Shen, W., Tahir, S. K., Thompson, C. B., Tomaselli, K. J., Wang, B., Wendt, M. D., Zhang, H., Fesik, S. W., and Rosenberg, S. H. (2005) An inhibitor of Bcl-2 family proteins induces regression of solid tumors. *Nature* **435,** 677–681
34. Couet, J., Li, S., Okamoto, T., Ikezu, T., and Lisanti, M. P. (1997) Identification of peptide and protein ligands for the caveolin-scaffolding domain: implications for the interaction of caveolin with caveolae-associated proteins. *J. Biol. Chem.* **272,** 6525–6533
35. Ahmed, N., Dasari, S., Srivastava, S. S., Sneh, A., Ahmad, A., Islam Khan, M., and Krishnasastry, M. V. (2008) Taxol and 10-deacetylbaccatin III induce distinct changes in the dynamics of caveolae. *FEBS Lett.* **582,** 3595–3600
36. MacKeigan, J. P., Collins, T. S., and Ting, J. P. (2000) MEK inhibition enhances paclitaxel-induced tumor apoptosis. *J. Biol. Chem.* **275,** 38953–38956
37. Seidman, R., Gitelman, I., Sagi, O., Horwitz, S. B., and Wolfson, M. (2001) The role of ERK 1/2 and p38 MAP-kinase pathways in taxol-induced apoptosis in human ovarian carcinoma cells. *Exp. Cell Res.* **268,** 84–92
38. Lee, L. F., Li, G., Templeton, D. J., and Ting, J. P. (1998) Paclitaxel (Taxol)-induced gene expression and cell death are both mediated by the activation of c-Jun NH_2-terminal kinase (JNK/SAPK). *J. Biol. Chem.* **273,** 28253–28260
39. Sunters, A., Madureira, P. A., Pomeranz, K. M., Aubert, M., Brosens, J. J., Cook, S. J., Burgering, B. M., Coombes, R. C., and Lam, E. W. (2006) Paclitaxel-induced nuclear translocation of FOXO3a in breast cancer cells is mediated by c-Jun NH_2-terminal kinase and Akt. *Cancer Res.* **66,** 212–220
40. Amato, S. F., Swart, J. M., Berg, M., Wanebo, H. J., Mehta, S. R., and Chiles, T. C. (1998) Transient stimulation of the c-Jun NH_2-terminal kinase/activator protein 1 pathway and inhibition of extracellular signal-regulated kinase are early effects in paclitaxel-mediated apoptosis in human B lymphoblasts. *Cancer Res.* **58,** 241–247
41. Boldt, S., Weidle, U. H., and Kolch, W. (2002) The role of MAPK pathways in the action of chemotherapeutic drugs. *Carcinogenesis* **23,** 1831–1838
42. Selimovic, D., Hassan, M., Haikel, Y., and Hengge, U. R. (2008) Taxol-induced mitochondrial stress in melanoma cells is mediated by activation of c-Jun N-terminal kinase (JNK) and p38 pathways via uncoupling protein 2. *Cell Signal.* **20,** 311–322
43. Blagosklonny, M. V. (2001) Paradox of Bcl-2 (and p53): why may apoptosis-regulating proteins be irrelevant to cell death? *Bioessays* **23,** 947–953
44. Ferlini, C., Raspaglio, G., Mozzetti, S., Distefano, M., Filippetti, F., Martinelli, E., Ferrandina, G., Gallo, D., Ranelletti, F. O., and Scambia, G. (2003) Bcl-2 down-regulation is a novel mechanism of paclitaxel resistance. *Mol. Pharmacol.* **64,** 51–58
45. Luo, D., Cheng, S. C., Xie, H., and Xie, Y. (2000) Effects of Bcl-2 and Bcl-XL protein levels on chemoresistance of hepatoblastoma HepG2 cell line. *Biochem. Cell Biol.* **78,** 119–126
46. Pawson, T., and Scott, J. D. (1997) Signaling through scaffold, anchoring, and adaptor proteins. *Science* **278,** 2075–2080
47. Sverdlov, M., Shajahan, A. N., and Minshall, R. D. (2007) Tyrosine phosphorylation dependence of caveolae-mediated endocytosis. *J. Cell Mol. Med.* **11,** 1239–1250
48. Tabuchi, Y., Matsuoka, J., Gunduz, M., Imada, T., Ono, R., Ito, M., Motoki, T., Yamatsuji, T., Shirakawa, Y., Takaoka, M., Haisa, M., Tanaka, N., Kurebayashi, J., Jordan, V. C., and Naomoto, Y. (2009) Resistance to paclitaxel therapy is related with Bcl-2 expression through an estrogen receptor-mediated pathway in breast cancer. *Int. J. Oncol.* **34,** 313–319